Entropy-driven stabilization of the cubic phase of MaPbI3 at room temperature

A. Bonadio[1], C. A. Escanhoela Jr[1], F. P. Sabino[1], G. Sombrio[1], V. G. de Paula[1], F. F. Ferreira, [1] A. Janotti[2], G. M. Dalpian[1], and J. A. Souza[1]

[1] *Universidade Federal do ABC, Santo André, SP, Brazil*

[2] *Department of Materials Science and Engineering, University of Delaware, DE, USA*

1. Results

1.1. X-ray diffraction

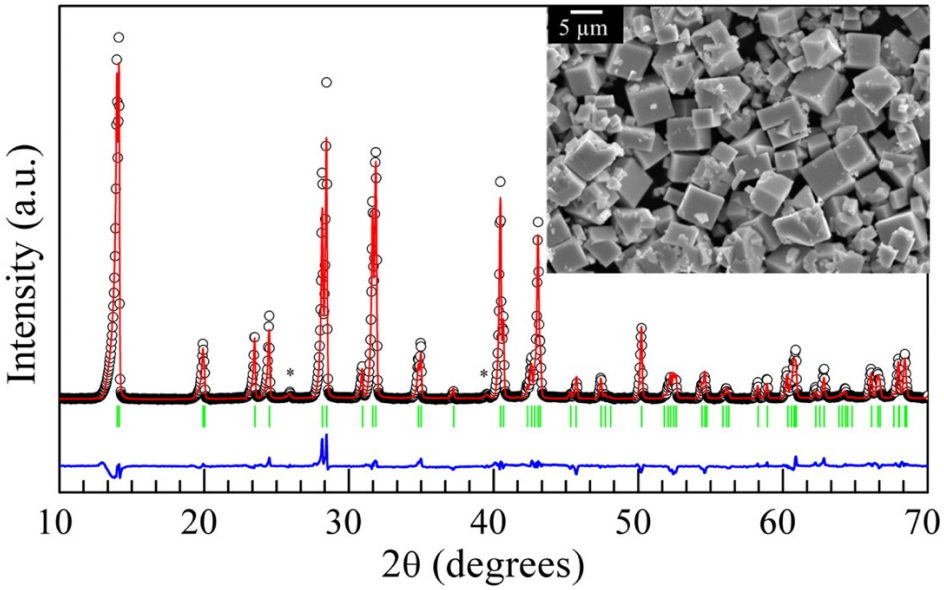

Figure S1 – X-ray powder diffraction of the $MAPbI_3$ sample synthesized by the solvothermal method. The asterisks indicate traces of 0.56% of the PbI_2 phase.

1.2. Scanning electron microscopy

The morphological studies of the samples were carried out by scanning electron microscopy (SEM) (JEOL JSM-6010LA). Figures S2, S3, S4, and S5 show the SEM images of the fractured surface of as-compacted (S0h) $MAPbI_3$ sample and samples annealed at 250 ºC during S10h, S20h, and S40h, respectively.

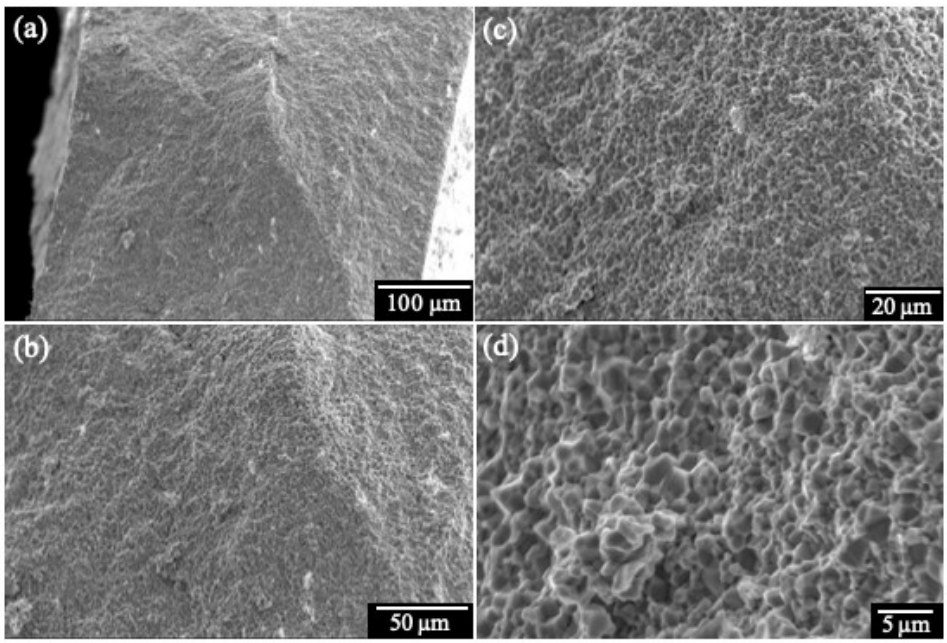

Figure S2 – Cross-sectional SEM images of the $MAPbI_3$ perovskite sample (S0h) with different magnifications.

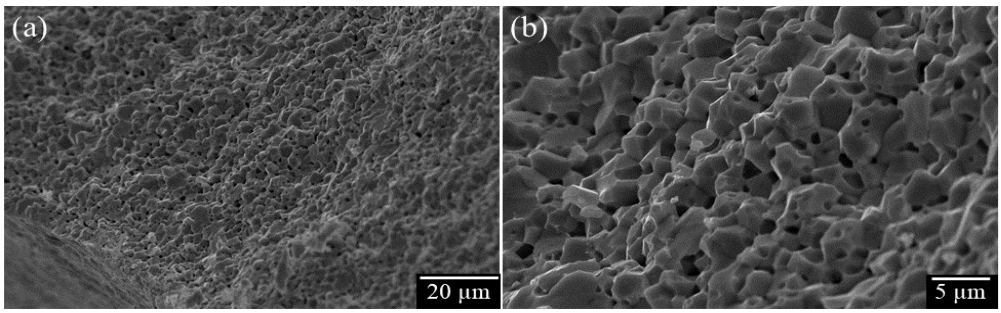

Figure S3 – Cross-sectional SEM images of the $MAPbI_3$ perovskite sample thermal annealed for 10 hours at 250 ºC (S10h) with different magnifications.

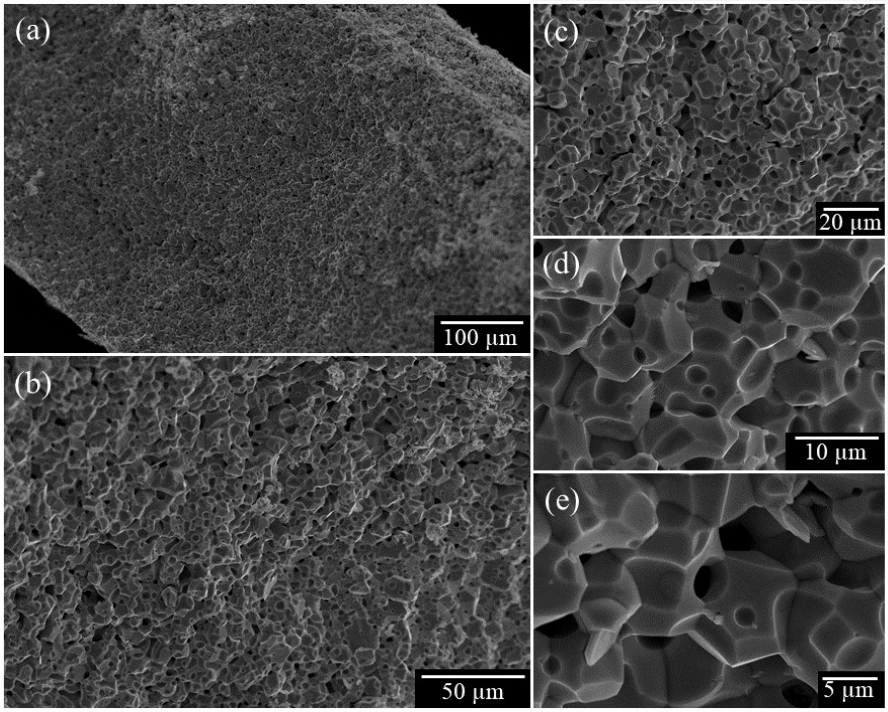

Figure S4 – Cross-sectional SEM images of the $MAPbI_3$ perovskite sample thermal annealed for 20 hours at 250 ºC (S20h) with different magnifications.

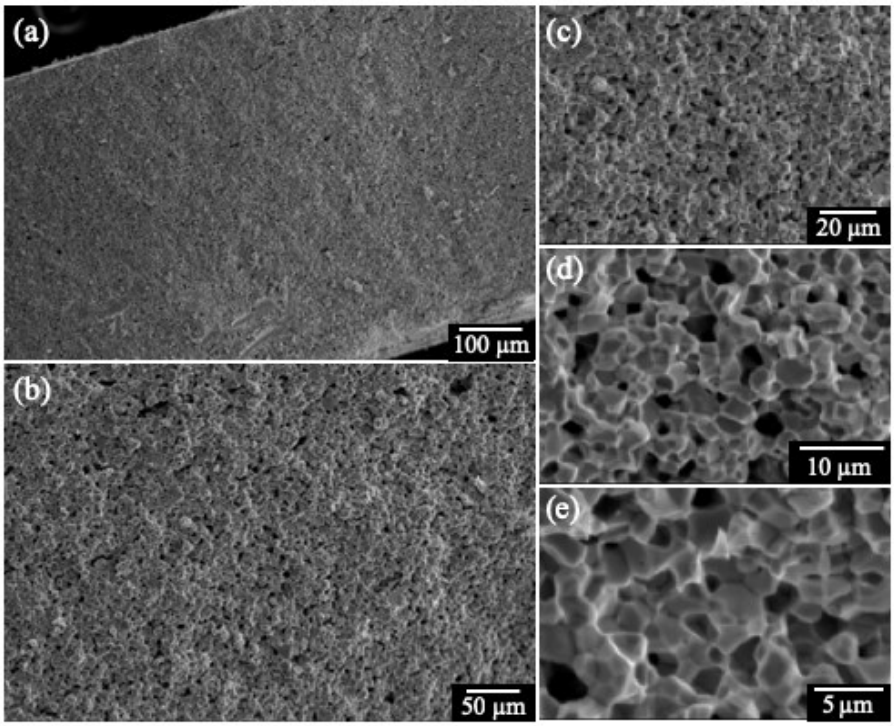

Figure S5 – Cross-sectional SEM images of the $MAPbI_3$ perovskite sample thermal annealed for 40 hours at 250 ºC (S40h) with different magnifications.

1.3. EDS analysis

The energy dispersive spectroscopy (EDS) analysis of S0h and S40h samples are presented in Fig. S6 and S7. The EDS spectrum shows the presence of Carbon, Nitrogen, Oxygen, Lead and Iodide. From the EDS map analysis, it can be noted that all the elements (C, N, Pb and I) are well distributed in the samples. From EDS analysis we can also determine the ratio of Pb and I atoms in the molecular formula to be 1Pb:3I for both samples, accordingly to Table 1 and 2, indicating that the stoichiometry has not changed. It is difficult to infer about the stoichiometry of samples from the C:N ratio of the organic fraction, although the percentage of N has remained the same for both samples. Oxygen and the excess of Carbon may be attributed to the impurities of the substrate and carbon tape used for this measurement, respectively.

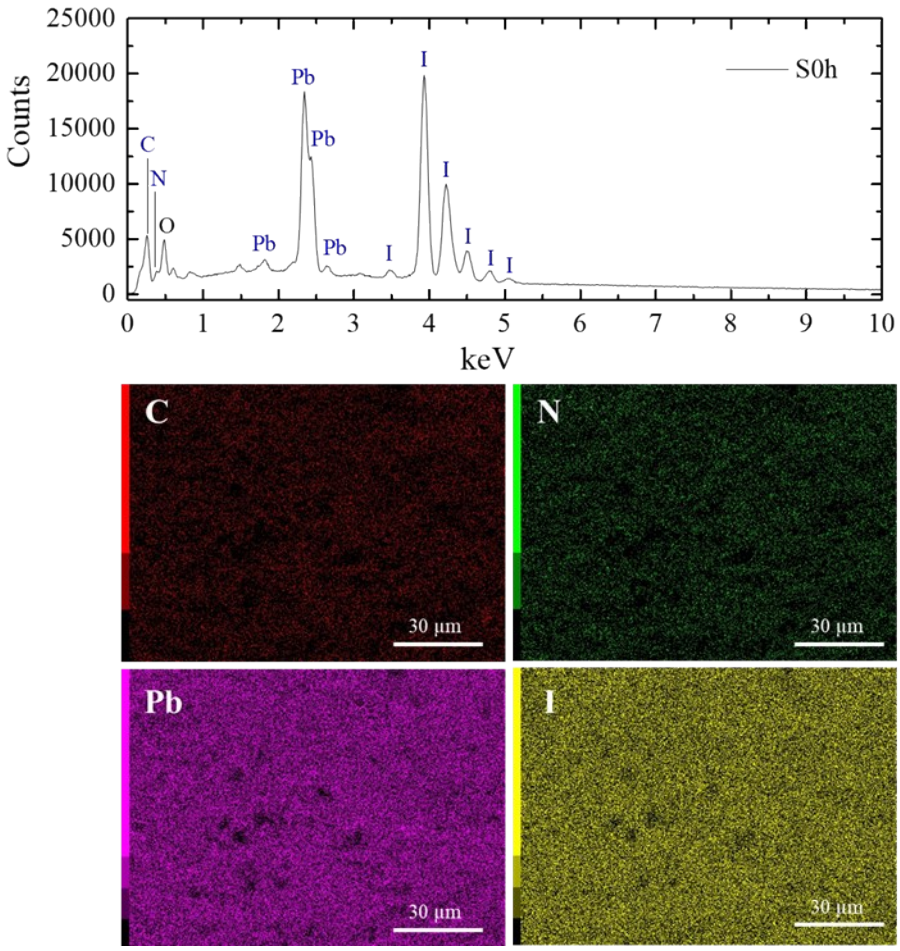

Figure S6 – (a) EDS spectrum and (b) corresponding EDS map analysis of the fractured surface of S0h sample.

Table S1 - Analysis of elements present on the fractured surface of S0h sample.

C (mol%)	N (mol%)	Pb (mol%)	I (mol%)
23.57 ± 0.04	3.64 ± 0.13	10.87 ± 0.38	61.92 ± 0.93

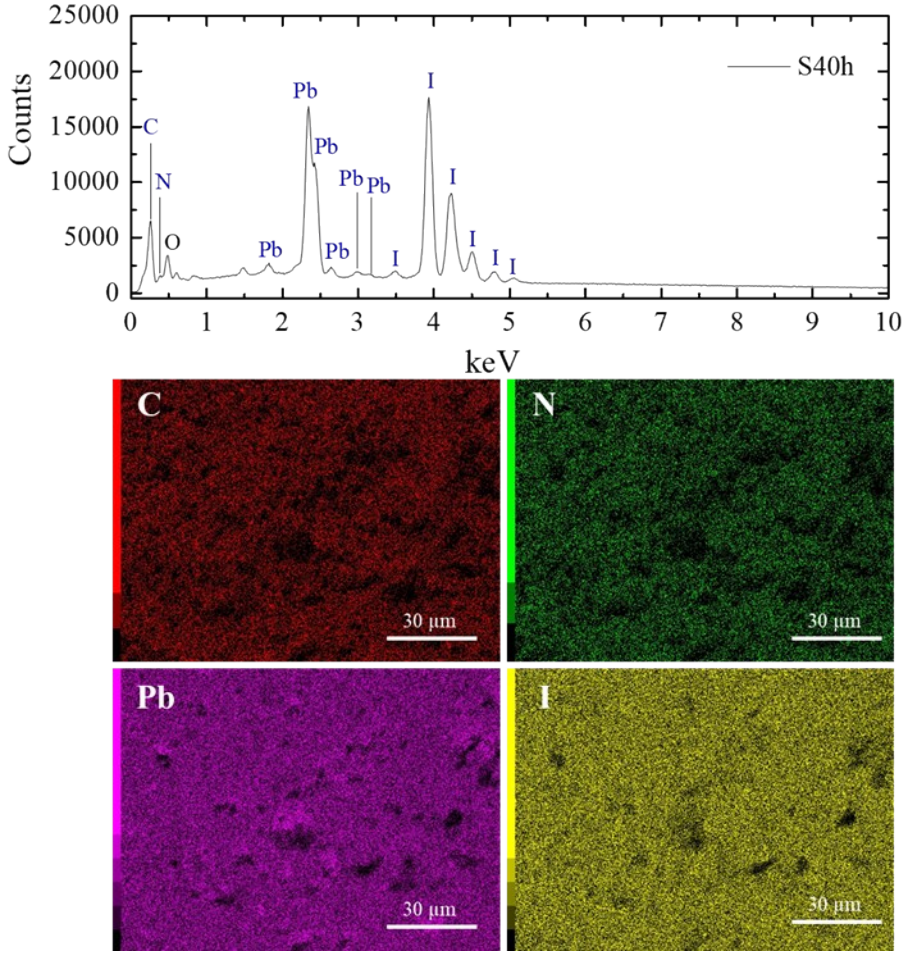

Figure S7 – (a) EDS spectrum and (b) corresponding EDS map analysis of the fractured surface of S40h sample.

Table S2 – Analysis of elements present on the fractured surface of S40h sample.

C (mol%)	N (mol%)	Pb (mol%)	I (mol%)
33.72 ± 0.04	3.60 ± 0.13	9.57 ± 0.37	53.10 ± 0.91

1.4. Infrared spectroscopy (IFTR)

The long annealing times allowed the evaporation of the chemical species from the pelletized samples. The FTIR spectra (Figure S8) indicated the presence of traces of $NH_4PbI_3{\cdot}(H_2O)_2$. On the basis of our results, and literature reports [1], the proposed thermal decomposition process of the pelletized $MAPbI_3$ perovskite is as follow:

$$CH_3NH_3PbI_3 + 2H_2O + NH_3\uparrow \xrightarrow{\Delta} NH_4PbI_3 \cdot (H_2O)_2 + CH_3NH_2\uparrow \quad (1)$$

The evaporation of this species during the annealing contributes to the formation of voids on the pelletized samples. Furthermore, the PbI_2 decomposition product is just found on the outer sample surface, which means that the lead iodide is thermally diffused through the sample.

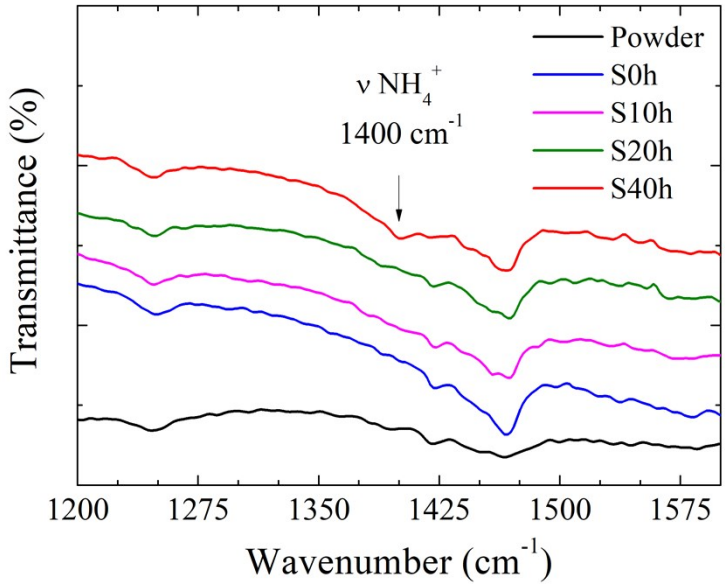

Figure S8 – Infrared spectra of the pelletized $MAPbI_3$ perovskite samples annealed at 250 ºC for t = 0, 10, 20, and 40 hours.

1.5. X-ray powder diffraction (XRPD) and Rietveld refinement analysis

The structural properties were studied by using X-ray powder diffraction (XRPD) and the Rietveld method [2], implemented in the TOPAS-*Academic* V.6 [3] software, which was used to refine the structural parameters and peak shapes from the XRPD patterns. The structural

refinement of the pelletized $MAPbI_3$ perovskite samples S0h and S10h was carried out by using the *I4/mcm* tetragonal space group symmetry. Figures S6 and S7 show the refined structural model of the samples S0h and S10h, respectively. With annealing times longer than 20 hours, the X-ray patterns showed a reduction of the Bragg reflection split, suggesting an increase of symmetry from *I4/mcm* tetragonal to a cubic $Pm\bar{3}m$. However, the refinement of the S20h and S40h samples using the $Pm\bar{3}m$ or *I4/mcm* space groups resulted in a poor quality of Rietveld fit and statistical parameters, as shown in Figures S8 and S9. For this reason, in the refinements of the S20h and S40h samples, we used a symmetry-mode decomposition, which was obtained using ISODISTORT[4]. The structural distortion modes of crystalline materials are induced by irreducible representations (*irrep*) of the parent space-group symmetry. In our case, the cubic ($Pm\bar{3}m$) to tetragonal (*I4/mcm*) transition is due to the special *R*-point (R_4^+), with the *k*-point in the reciprocal space $k = [½, ½, ½]$; the cubic-to-tetragonal transition can be represented by the R_4^+ rotational distortion mode amplitude. Figures S10 and S11 show the best fit to the experimental diffraction patterns using the distortion mode amplitude for samples S20h and S40h. Tables 1 and 2 summarize the *R*-factors for different space groups.

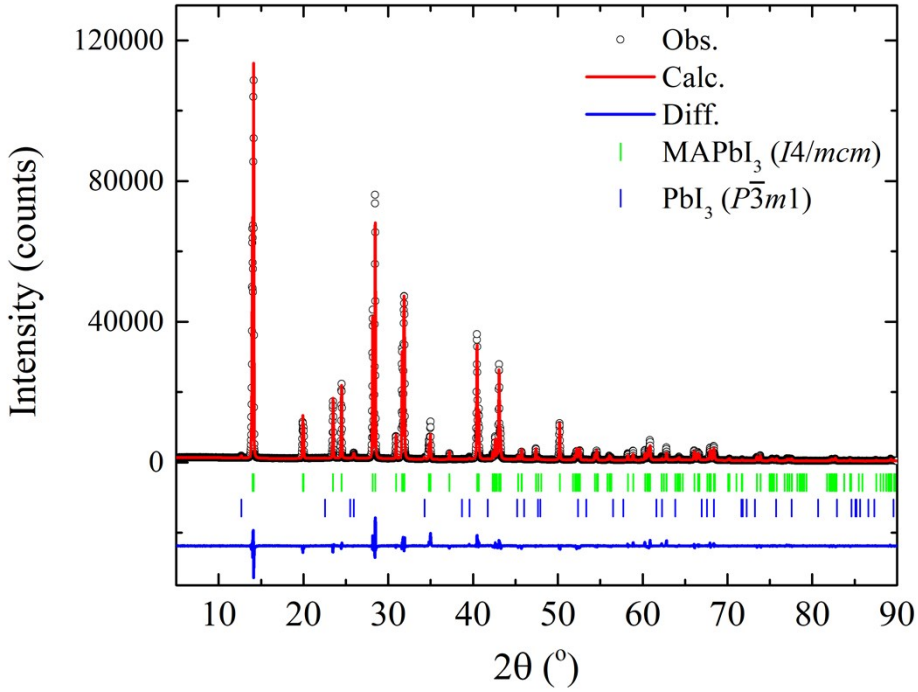

Figure S9 – Rietveld plot of the as-compacted $MAPbI_3$ (S0h) sample at room temperature. Black circles indicate the observed intensities, and the red line shows the calculated profile. The blue line at the bottom displays the difference between the observed and calculated patterns. Tick marks stand for the Bragg peaks of both $MAPbI_3$ and PbI_3 phases.

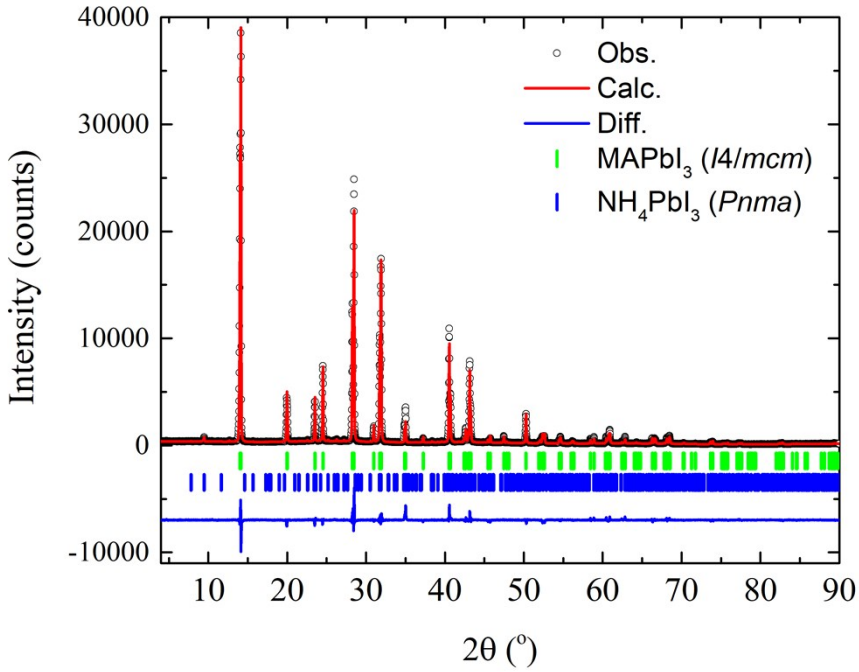

Figure S10 – Rietveld plot of the 10-h-annealed at 250 ºC $MAPbI_3$ (S10h) sample at room temperature. Black circles indicate the observed intensities, and the red line shows the calculated profile. The blue line at the bottom displays the difference between the observed and calculated patterns. Tick marks stand for the Bragg peaks of both $MAPbI_3$ and PbI_3 phases.

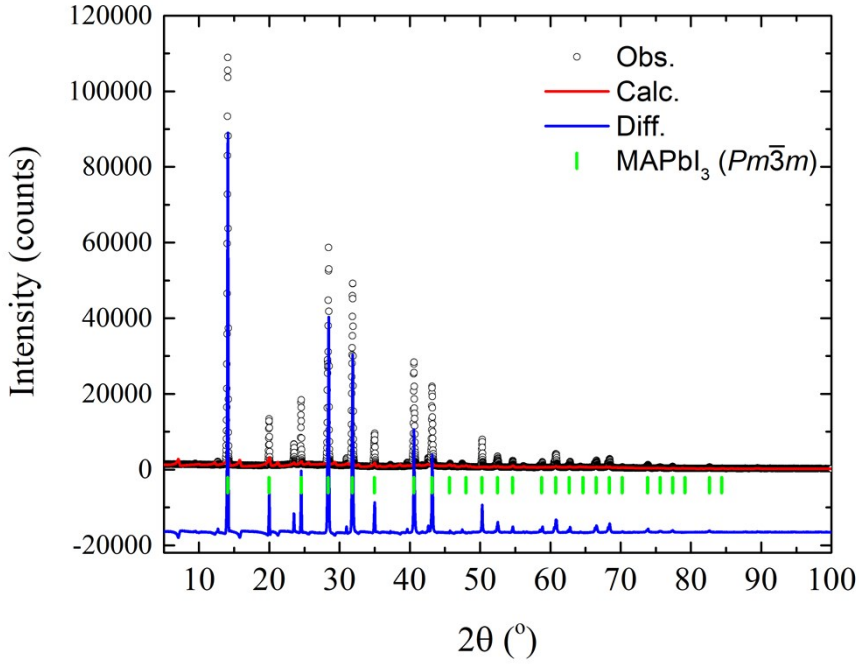

Figure S11 – Rietveld plot of the 20-h-annealed at 250 ºC $MAPbI_3$ (S20h) sample at room temperature in the $Pm\bar{3}m$ space group. Black circles indicate the observed intensities, and the red line shows the calculated profile. The blue line at the bottom displays the difference

between the observed and calculated patterns. Tick marks stand for the Bragg peaks of the $MAPbI_3$ phase.

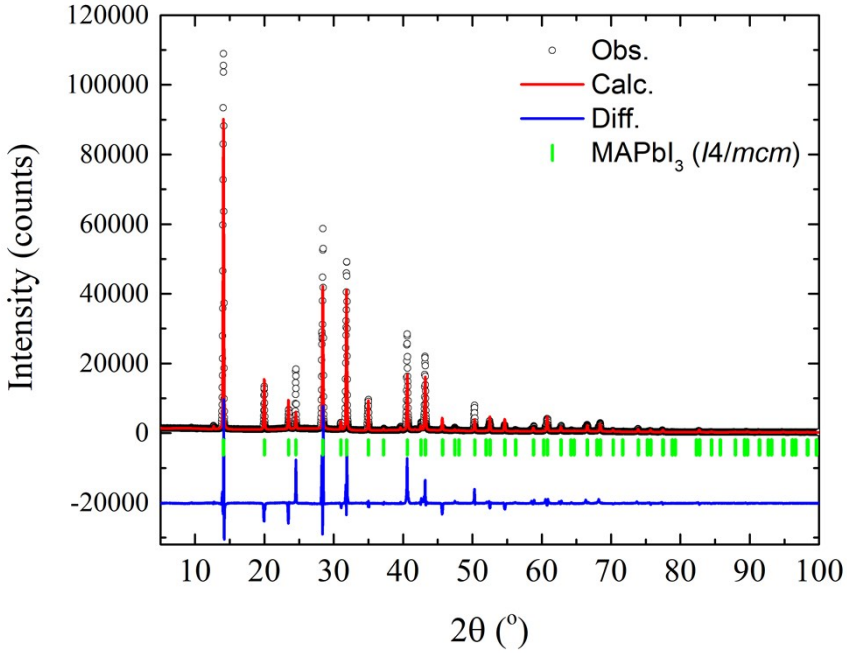

Figure S12 – Rietveld plot of the 20-h-annealed at 250 ºC $MAPbI_3$ (S20h) sample at room temperature in the *I*4/*mcm* space group. Black circles indicate the observed intensities, and the red line shows the calculated profile. The blue line at the bottom displays the difference between the observed and calculated patterns. Tick marks stand for the Bragg peaks of the $MAPbI_3$ phase.

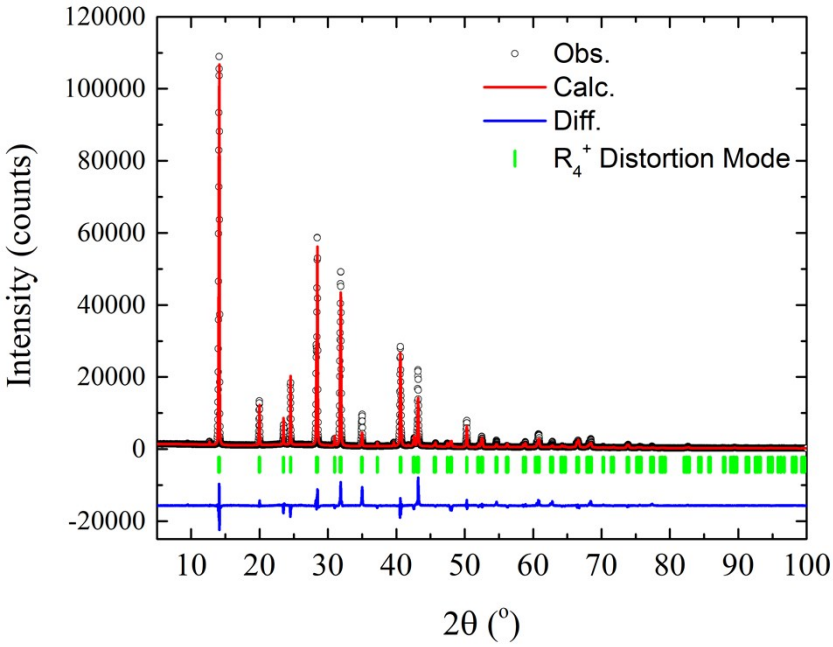

Figure S13 – Rietveld plot of the 20-h-annealed at 250 ºC $MAPbI_3$ (S20h) sample at room temperature in the *I*4/*mcm* space group with R_4^+ distortion mode. Black circles indicate the observed intensities, and the red line shows the calculated profile. The blue line at the bottom displays the difference between the observed and calculated patterns. Tick marks stand for the Bragg peaks of the $MAPbI_3$ phase.

Table S4 – Statistical *R*-factors, R_{Bragg} and R_{wp}, for the pelletized sample $MAPbI_3$ submitted to 20 hours of thermal annealing at 250 ºC with different space groups and applying R_4^+ distortion mode.

	Sample S20h space group refinement		
	Pm$\underline{3}$*m*	*I*4/*mcm*	*I*4/*mcm* and R_4^+ distortion mode
R_{Bragg}	59.3	20.4	9.1
R_{wp}	59.7	26.1	6.8

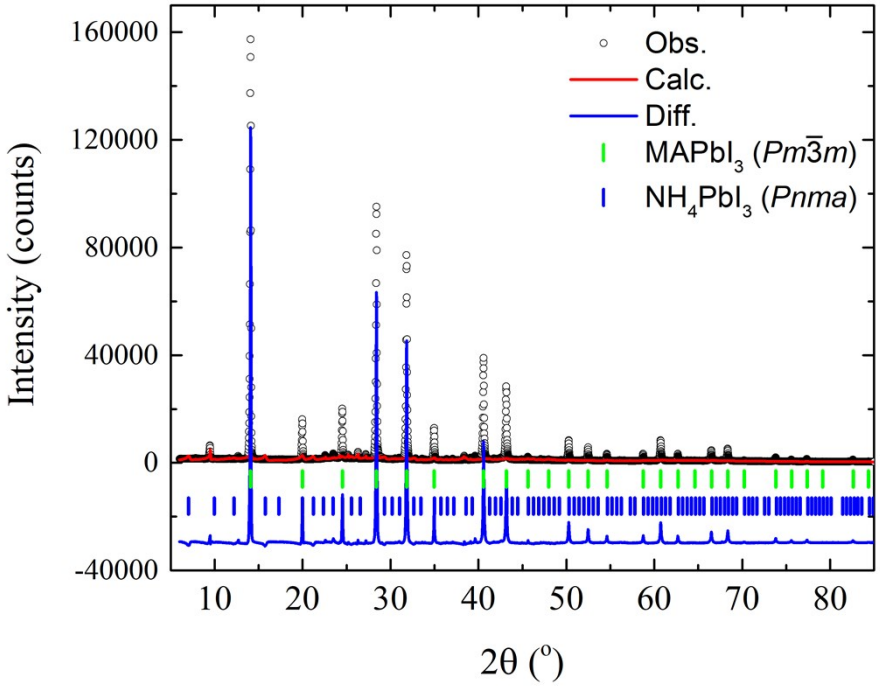

Figure S14 – Rietveld plot of the 40-h-annealed at 250 ºC $MAPbI_3$ (S40h) sample at room temperature in the $Pm\bar{3}m$ space group. Black circles indicate the observed intensities, and the red line shows the calculated profile. The blue line at the bottom displays the difference between the observed and calculated patterns. Tick marks stand for the Bragg peaks of both the $MAPbI_3$ and NH_4PbI_3 phases.

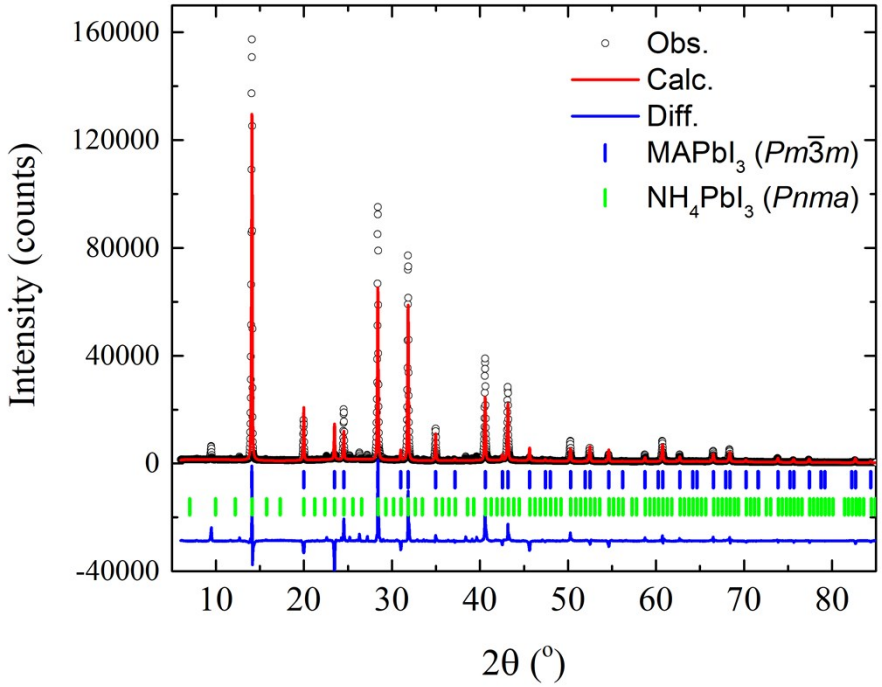

Figure S15 - Rietveld plot of the 40-h-annealed at 250 ºC $MAPbI_3$ (S40h) sample at room temperature in the $Pm\bar{3}m$ and *Pnma* space groups. Black circles indicate the observed intensities, and the red line shows the calculated profile. The blue line at the bottom displays the difference between the observed and calculated patterns. Tick marks stand for the Bragg peaks of both the $MAPbI_3$ and NH_4PbI_3 phases.

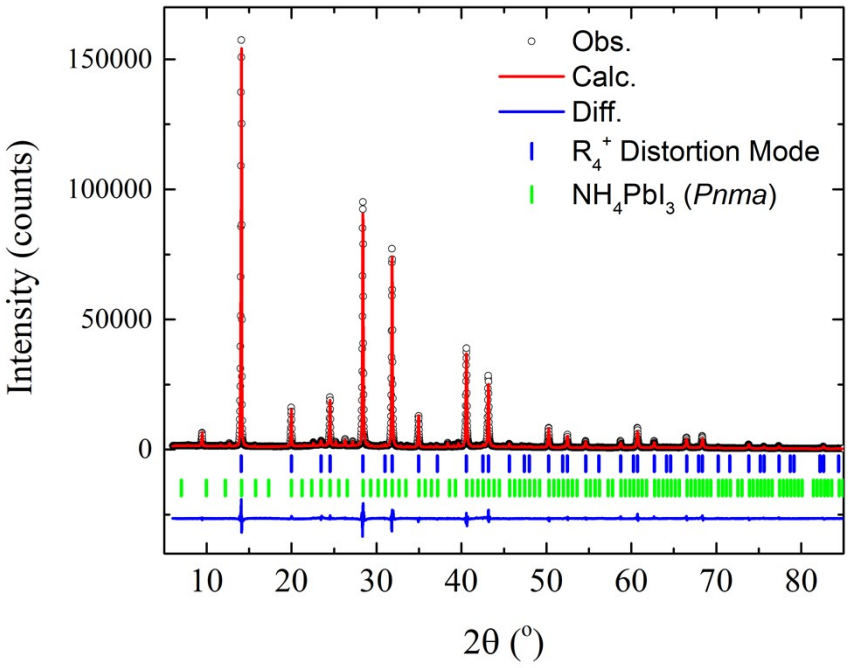

Figure S16 – Rietveld plot of the 20-h-annealed at 250 ºC $MAPbI_3$ (S20h) sample at room temperature in the *I*4/*mcm* with the R_4^+ distortion mode and *Pnma* space groups. Black circles indicate the observed intensities, and the red line shows the calculated profile. The blue line at the bottom displays the difference between the observed and calculated patterns. Tick marks stand for the Bragg peaks of both the $MAPbI_3$ and NH_4PbI_3 phases.

Table S5 – Statistical factors, R_{Bragg} and R_{wp}, for the pelletized sample MAPbI3 submitted to 40 hours of thermal annealing at 250 ºC with different space groups and applying R_4^+ distortion mode.

	Sample S40h space group refinement		
	$Pm\bar{3}m$	*I*4/*mcm*	*I*4/*mcm* and R_4^+ distortion mode
R_{Bragg}	63.2	17.9	3.1
R_{wp}	62.1	26.9	7.4

References

[1] I. Deretzis *et al.*, "Atomistic origins of $CH_3NH_3PbI_3$ degradation to PbI_2 in vacuum," *Appl. Phys. Lett.*, vol. 106, no. 13, p. 131904, Mar. 2015, doi: 10.1063/1.4916821.

[2] H. M. Rietveld, "A profile refinement method for nuclear and magnetic structures," *J. Appl. Crystallogr.*, vol. 2, no. 2, pp. 65–71, Jun. 1969, doi: 10.1107/S0021889869006558.

[3] A. A. Coelho, "*TOPAS* and *TOPAS-Academic* : an optimization program integrating computer algebra and crystallographic objects written in C++," *J. Appl. Crystallogr.*, vol. 51, no. 1, pp. 210–218, Feb. 2018, doi: 10.1107/S1600576718000183.

[4] B. J. Campbell, H. T. Stokes, D. E. Tanner, and D. M. Hatch, "*ISODISPLACE* : a web-based tool for exploring structural distortions," *J. Appl. Crystallogr.*, vol. 39, no. 4, pp. 607–614, Aug. 2006, doi: 10.1107/S0021889806014075.